Hall thruster ion-induced sputtering of facility surfaces: Review of PMI data

IEPC-2024-532

Presented at the 38th International Electric Propulsion Conference, Toulouse, France
June 23-28, 2024

Saptarshi Biswas*, Richard A. Obenchain†, Ryan W. Cowan†
Oregon State University, Corvallis, OR, 97331, USA

Richard E. Wirz‡§
University of California, Los Angeles, Los Angeles, CA, 90095, USA
Oregon State University, Corvallis, OR, 97331, USA

Facility sputtering can obfuscate ground test results for high-powered, long-lifetime space propulsion systems. This paper reviews the ion-induced sputtering plasma material interactions (PMI) data for vacuum facility materials such as graphite, stainless steel, and aluminum for Hall thruster relevant ion energies 100 eV–1600 eV for the change landscape of propellant options by including xenon, krypton, and argon. A simple facility sputtering model provides context for the key parameters for ion-induced sputtering erosion and deposition. For these energies, the most data was found for Xe ion bombardment of carbon-based materials but with a high level of variance within material types, across material types, and for difference surface conditions. A relatively small amount of data for Xe on aluminum and iron (as a surrogate for stainless steel) were found. Similarly, little data was found for krypton and argon at Hall thruster relevant energies, particularly at non-zero incidence angles and energies within 1– keV. These results suggests that the electric propulsion (EP) community needs to continue to develop PMI data and models for EP-relevant facility effects across propellant and material options

Nomenclature

d	= distance from thruster to target [m]	J	= Current [A]
dA_i	= differential surface (m)	K	= incident ion energy [eV]
e	= electron charge, $1.6x10^{-19}C$	M	= Atomic weight [g/mol]
m	= mass per particle [kg]	T	= Temperature [K]
$\dot{m}_a$	= anode mass flow rate (mg/s)	V	= Potential [V]
n	= particle count [#]	Z	= Atomic number [-]
$\dot{n}$	= particle flow rate [#/s]	ρ	= material density $[kg/m^3]$
r	= radius from thruster centerline [m]	θ, ϕ	= angle [radians]
s	= erosion depth [m]	$\Gamma_{i,reflected}$	= flux reflected from surface i $(1/(\mathrm{m}^2\,\mathrm{s}))$
$\dot{s}$	= erosion rate [m/s]	$\Gamma_{i,adsorbed}$	= flux adsorbed by surface i $(1/(\mathrm{m}^2\,\mathrm{s}))$
y	= total sputtered particles [#]	$P()$	= Normalized beam profile function []
A	= Area $[m^2]$	$Y()$	= Sputtering yield function [atoms/ion]
E	= Ion energy [eV]		

*Postdoctoral Scholar, College of Engineering, saptarshi.biswas@oregonstate.edu
†Graduate Research Assistant
‡Adjunct Professor, Mechanical and Aerospace Engineering, wirz@ucla.edu
§Boeing Professor, Executive Director of Aerospace Research Programs, College of Engineering, richard.wirz@oregonstate.edu

I. Introduction

A high-powered, long-lifetime electric propulsion (EP) system is crucial for space exploration, necessitating ground-based testing to simulate the space environment. One major challenge in these tests is plume impingement, where ions from the propulsion system interact with vacuum facility surfaces of materials such as stainless steel and aluminum.[1–4] Despite the relatively low energy of many of these ions ($\leq$ 1 keV), they can still cause substantial erosion of the facility walls over prolonged test duration, which can contaminate the thruster undergoing experiment via back sputtering, particle transport, and redeposition on thruster surfaces. To mitigate these effects, vacuum chambers are often lined with sputter-resistant materials like graphite to address sputtering issues;[5] while reduced in comparison to other materials such as metals, however, graphite can undergo sputtering, transport, and redeposition when bombarded with ions from the thruster, thus affecting the thruster's performance.[6–8] Hence, analyzing the interaction of facility contaminants with the thruster during testing is vital, as these interactions can significantly impact thruster performance and lifetime estimates.[9–11] A recent study by Sabiston and Wirz,[12] with supporting evidence from Cowan et al.,[13] shows that the stainless steel facility walls, even if at high plume angles, may contribute significantly to sputtering/deposition behavior and the related uncertainty for Hall thruster ground testing. Additionally, as reported by Franz and Wirz,[14] the interplay between sputtering of material surfaces and the implantation/ejection and scattering of incident ions is critical to EP facility effects. These observations affect the accuracy of analyses related to sputtering/deposition[12,13] and facility backpressure.[15,16]

This paper builds on previous experimental and analytical reviews on the sputtering behavior of graphite when bombarded with Xe ions.[17–19] The topic is expected to continue evolving as new data and methods become available. Previous literature has led to the understanding that surface topology and grain orientation play a significant role in the sputtering behavior of materials,[20] with pyrolytic graphite offering higher purity and better crystallinity than synthetic graphite. Additionally, incidence angles and surface roughness significantly affect sputtering yields.[21–23] Ion implantation also plays a crucial role in sputtering,[14,24,25] and the results of different-sized ions impacting EP facility materials need further examination. Residual gases like oxygen and nitrogen can also significantly impact sputtering yields,[26] suggesting the importance of using internally mounted Residual Gas Analyzers (RGAs) to monitor species flux from different parts of the chamber to characterize the beam target environment and improve data repeatability. For graphite, sp^2 to sp hybridization occurs during ion bombardment,[27] leading to sputtering from those regions. Understanding other macroscopic effects, such as local heating and its impact on bond transformation, is crucial for developing comprehensive models of sputtering behavior.

Moreover, examining the sputtering behavior of Kr and Ar ions is essential with the increasing use of cheaper propellant alternatives as depicted in Table 1. In addition, the sputtering behavior of other vacuum facility materials, such as steel and aluminum, when bombarded by Xe, Ar, and Kr ions at various energies, incidence angles, surface roughness, fluence, and other parameters must be considered to develop a comprehensive knowledge of sputtering behavior induced by EP propellants on vacuum testing facilities. By identifying gaps in current understanding, extending the analysis to different materials, and documenting discrepancies, the goal is to develop a robust framework to understand facility interactions during ground-based Hall Effect Thruster (HET) testing.

Table 1: Comparison of Different EP Noble Gas Propellant Options

Propellant	At wt, (g/mol)	E_i (eV)	M/E_i	Price, €/L	Density, g/L	€/kg	Relative cost vs. Ar	T_c
Xe	**131.3**	**12.13**	**10.82**	**25**	**5.89**	**4240**	**1905**	**165.03 K**
Kr	**83.8**	**14.00**	**5.98**	**3**	**3.75**	**800**	**359**	**119.93 K**
Ar	**39.9**	**15.81**	**2.53**	**0.0036**	**1.78**	**2.23**	**1**	**87.35 K**
Ne	*20.2*	*21.64*	*0.93*	*0.504*	*0.9*	*560*	*251*	*27.15 K*
He	*4.0*	*24.59*	*0.16*	*0.0061*	*0.18*	*37.8*	*17*	*4.25 K*

For consistency, the recent H9 test campaign conducted within the VTF-2 facility at the High Power Electric Propulsion Laboratory at Georgia Institute of Technology as part of the JANUS (Joint Advanced Propulsion Institute) is used as a reference experiment. The facility materials include stainless steel 304

and polycrystalline graphite located at various positions and incident angles relative to the krypton-fed H9 thruster. A reduced order model is presented to predict the erosion and deposition rates of materials used in the vacuum facility and to highlight the importance of specific experimental parameters to sputtering calculations. This model provides a theoretical prediction for the experimental observations obtained from sputtering data of Kr ions on stainless steel and graphite at different angles and exposure durations.[28]

Overall, this paper aims to enhance the accuracy and reliability of sputtering predictions and cite missing or sparse data within the community, thereby improving the testing conditions and performance assessment of Hall thrusters.

II. Methodology

A. Approach

Understanding material response to ion bombardment is crucial for erosion and deposition analysis. Notably, we need to know how sputtering affects the performance of thrusters and how it can lead to redeposition of sputtered material on the thruster surfaces.[12] To achieve this, we must study the sputtering yield of vacuum facility materials caused by EP-relevant propellants. To fill the gap in existing research on the sputtering of vacuum chamber materials, we conducted a comprehensive literature survey on sputtering yields using alternative propellants like krypton and argon and compare them with existing literature on xenon with the goals of summarizing previous studies, identifying critical parameters, and pinpointing gaps in knowledge about the sputtering of carbon, stainless steel, and aluminum when bombarded by xenon, krypton, and argon ions within the 1 keV range. We then compared the sputtering yields from the literature for various facility surfaces and analyze the trends for each material. We also performed a first-order estimate of the JANUS test campaign in terms of erosion and deposition of facility materials of VTF-2 using the reduced order model in the following section.

B. Reduced Order Model for Sputtering

Multiple variations of analytical sputtering and deposition models have been published. One recent comprehensive example was presented by Lobbia et al. in 2019,[6] which leveraged yield measurements conducted by Williams et al. previously.[29] As with most such efforts, the analytical model generally uses thruster operating parameters to determine the energy, fluence, and beam profile for the given domain, then applies integration of an experimentally-derived PDF over the specific target surface or segment in question to generate sputterant yields. These are then projected back to the deposition surface using a view factor model of particle transport.

To assess the impact of various parameters on erosion depth for a given material, we use an analytical sputtering model. This model was used for witness and target plate positioning during the recent JANUS Hall Effect Thruster Experiment at the HPEPL VTF-2 Facility at Georgia Tech.[28]

For a given number of ions n_i of equal energy K_i incident on a region of interest at angle θ_i, sputtering yield in particles is therefore:

$$y = n_i Y(\theta_i, K_i) \tag{1}$$

If the region is normal to the incoming ions and has area A_s, the average particle yield per unit area is:

$$y_{avg} = \frac{n_i}{A_s} Y(\theta_i, K_i) \tag{2}$$

If the regional density of the sputtered surface is ρ_s and mass per particle is m_s, we can determine the average erosion depth over the region s_avg as:

$$s_{avg} = \frac{m_s n_i}{\rho_s A_s} Y(\theta_i, K_i) \tag{3}$$

Taking the time derivative of both sides, the average rate of erosion for the region is:

$$\dot{s}_{avg} = \frac{m_s \dot{n}_i}{\rho_s A_s} Y(\theta_i, K_i) \tag{4}$$

In predicting erosion rates, the four values ρ_s, $\dot{n}_i$, A_s, and $Y(\theta_i, K_i)$ become the quantities of interest.

Significant research effort has been made in determining $Y(\theta_i, K_i)$ for various combinations of incident ions and surface materials. For reduced order calculations, we seek to simplify the impact of both the incident angle and the ion energy; luckily, reasonable approximations for both can be made.

For any surface of finite area with a local surface roughness that is significantly larger than the atomic diameter of the incident ion, local surface geometry will mitigate the effects of incident angle on the resulting yield. As such, a reasonable approximation of total yield can be made by assuming normal incidence ($\theta_i = 0\,\text{deg}$) regardless of the angle to the thruster.[12,14] For thruster test facilities, local surface roughness is generally reported by manufacturers on the order of microns, while the atomic radii of propellant ions are on the order of nanometers or less; thus, the normal incidence approximation should hold.

$$Y(\theta_i, K_i) \approx Y_0(K_i) \tag{5}$$

Polk recently conducted a thorough analysis of the effects of multiply charged ion species on true vs calculated yield rates.[17] For singly-charged ion energies in the range used for thruster testing (generally 300 eV or higher), yields generally increase linearly with ion charge:

$$Y(\theta_i, K_{++}) \approx 2Y_0(K_+), Y(\theta_i, K_{+++}) \approx 3Y_0(K_+) \tag{6}$$

For a beam composed of singly-, doubly-, and triply-charged ions, the particle flow rate can be summarized as:

$$\dot{n}_i = (\dot{n}_{i+} + \dot{n}_{i++} + \dot{n}_{i+++}) \tag{7}$$

In terms of yield:

$$\dot{y}_i = \dot{n}_i Y_0(K_i) = (\dot{n}_{i+} Y_0(K_i+) + \dot{n}_{i++} Y_0(K_{i++}) + \dot{n}_{i+++} Y_0(K_{i+++})) \tag{8}$$

$$\dot{y}_i = (\dot{n}_{i+} Y_0(K_i+) + 2\dot{n}_{i++} Y_0(K_i+) + 3\dot{n}_{i+++} Y_0(K_i+)) \tag{9}$$

For electron charge $e = 1.6x10^{-19}C$:

$$\dot{y}_i = \frac{1}{e} Y_0(K_i+)(e\dot{n}_{i+} + 2e\dot{n}_{i++} + 3e\dot{n}_{i+++}) \tag{10}$$

Current per species J_{ix} is defined as the particle flow rate times the charge per particle. Therefore, we can state yield rate in terms of currents:

$$\dot{y}_i = \frac{1}{e} Y_0(K_i+)(J_{i+} + J_{i++} + J_{i+++}) \tag{11}$$

We can approximate the yield rate based on the total ion current to the surface and the normal yield for a singly-charged ion.

$$\dot{y}_i = \frac{J_i}{e} Y_0(K_i+) \tag{12}$$

For K_{i+}, a reasonable value is to use the accelerating potential for the thruster, V_a. Thus we end with yield and erosion rates of:

$$\dot{y}_i = \frac{J_i}{e} Y_0(V_a) \tag{13}$$

$$\dot{s}_{avg} = \frac{m_s J_i}{e\rho_s A_s} Y_0(V_a) \tag{14}$$

While the beam current itself must be measured experimentally, HET mass flow is often adjusted slightly during experimental testing to achieve a target beam current. Thus, the use of current in this reduced-order model is preferable to using flow rate.

Most presented beam profiles are two dimensional: current (either cumulative or instantaneous) as a function of an angle from the thruster axis. The profile may be left in raw measurements of current, normalized for the total current in the linear sample or normalized to the total beam current measured from the thruster. Conversion from a two-dimensional beam profile to a three-dimensional profile (current as a function of two angles or, alternatively, as a function of a solid angle in steradians or degrees squared) requires interpretation of the specific profile provided, which can vary widely depending on the source and method of generation. For the purposes of reduced order sputtering calculations, we assume a measurement

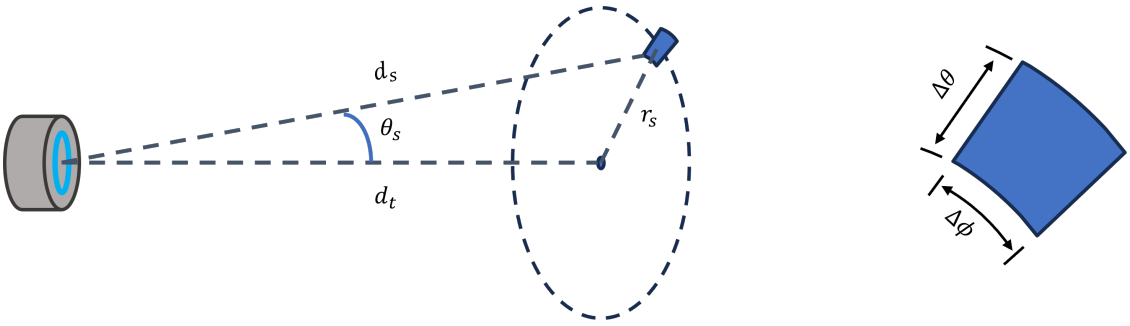

Figure 1: To determine the incident ions for a specific region (shaded blue), we project a circle of radius r_s and circumference angle θ_s a distance of d_t from the thruster face, with the finite region area given the angular dimensions of $\Delta\theta$ and $\Delta\phi$.

taken at a location that can be described by a local area A_s and an angle from thruster centerline θ_s as shown in Figure 1. If the angular span of the surface is small – that is, if $\Delta\theta$ is on the order of one degree or less – then the total current to the surface can be calculated directly from the beam profile. If the beam profile is given as normalized to the total beam current and as a function $P_b(\theta_s) = [rad^{-2}]$, then the incident current to the surface is calculated as:

$$J_i = J_b P_b(\theta_s)\Delta\theta\Delta\phi \tag{15}$$

The area of the surface can be approximated as:

$$A_s = d_S sin(\theta_s)\Delta\phi * (d_s sin(\theta_s + \frac{\Delta\theta}{2}) - d_s sin(\theta_s - \frac{\Delta\theta}{2}) = 2d_t r_s sin(\frac{\Delta\theta}{2})\Delta\theta \tag{16}$$

The last quantity of interest is the density of the surface material, ρ_s. This is generally a property of the material of the surface, though certain materials may amorphized to higher densities under sufficient fluence.[14,30] Returning to our modified equation:

$$\dot{s}_{avg} = \frac{m_s}{e\rho_s}\frac{J_i}{A_s}Y_0(V_a) \tag{17}$$

The first term isolates the constants of the system. In the most convenient form, the second term equates as:

$$\frac{J_i}{A_s} = \frac{J_b P_b(\theta_s)\Delta\theta\Delta\phi}{2d_t r_s sin(\frac{\Delta\theta}{2})\Delta\theta} = \frac{2J_b P_b(\theta_s)}{2d_t r_s}\frac{\frac{\Delta\theta}{2}}{sin(\frac{\Delta\theta}{2})} \approx \frac{J_b P_b(\theta_s)}{2d_t r_s} \tag{18}$$

$$\therefore \dot{s}_{avg} = \frac{m_s}{e\rho_s}\frac{J_b P_b(\theta_s)}{d_t r_s}Y_0(V_a) \tag{19}$$

This ROM considered four key parameters for sputtering calculations: an angularly resolved beam profile, surface material density, surface area, and the yield function. The first three parameters are generally well-characterized or inputs as part of a given experimental effort; the final parameter, the yield function, contains the largest uncertainty in terms of known quantities and application to specific experimental studies. Coupling these observations with the DSMC modeling by Sabiston and Wirz[12] and Franz and Wirz,[14] we note sputtering behavior is highly dependent on local incident angle, distance from the ion source, and angle with respect to the ion source. Additionally, the 3-dimensional PDF sputtering profile is required to accurately determine the deposition rates of sputtered material on the thruster and facility surfaces. These observations strongly motivate the need for accurate sputtering data, models, and analyses for EP propellants and facility material options.

III. Results and Discussion

Sputtering yield for vacuum facility-relevant materials as a function of ion incident energy is surveyed and plotted for EP-propellants like Xe, Kr, and Ar. To estimate repeatable sputter yield data, three of the important parameters need to be calibrated for an ion source - ion energy, ion incidence angle, and flux (current density). In the following section, we will focus on the first two parameters.

A. Normal Incidence

Sputtering yield for vacuum facility-relevant materials as a function of ion incident energy within 1000 eV is surveyed and plotted for EP-propellants like Xe, Kr, and Ar in Figs. 2, 4, and 5. Fig. 2 highlights the need for more stainless steel data with Xe bombardment. Although relevant literature exists on iron sputtering induced by noble gases, it only partially represents stainless steel, which comprises approximately 70% iron. Additionally, there is a noticeable scarcity of aluminum sputtering data within the energy domain relevant to Hall effect thruster regimes, typically below 1000 eV. This domain is critical for space propulsion applications where understanding material erosion rates is vital for longevity and performance. Contrastingly, the heavily researched area of ion-induced sputtering of carbon-based materials as depicted in Fig. 3 reveals systemic errors due to variations in testing conditions, indicating a need for better characterization and standardized methodologies.

The detailed analysis of sputtering yields further emphasizes the significant structural differences among carbon-based materials. Hechtl's[20] work reveals that pyrolytic graphite's sputtering yield is higher for grains parallel to the net plane than those perpendicular. Williams' work on PVD infiltrated and pyro-coated C-C composites exhibits similar sputtering behavior to pyrolytic graphite, suggesting consistency across different preparation methods. Deltschew's[31] study observed that direct exposure of carbon fibers to ion beams, where ions strike cylindrical fiber surfaces at various angles, produces higher sputter yields than graphite. This observation differs from Williams'[29] findings on PVD infiltrated pyro-coated C-C composites, which show more similar sputtering behavior with graphite. Kolasinski's[32] amorphous carbon data presents notable differences, likely due to the unique structure and testing methods, which include sensitive in situ mass loss measurements using quartz crystal microbalances. Polk's work[17] also highlights various systemic errors in sputtering yield measurements stemming from differences in experimental setups, ion beam sources, and material properties. For instance, half of the experimental setups used plasma sources while others used ion beam sources, each with advantages and disadvantages, such as high fluxes versus lower fluxes and variable incidence angles. Additionally, the methods for measuring the amount of sputtered material, whether by mass loss or quartz crystal microbalances, introduce variability and potential biases. These findings underscore the complexity and variability in sputtering behavior among different materials and highlight the need for comprehensive studies to inform material selection and usage in space propulsion systems.

Figures 4 and 5 show that the sputtering yield increases with ion incident energy for both Kr and Ar ions across various materials, including aluminum, iron, and carbon-based materials. Aluminum exhibits a nearly linear increase in yield with ion energy for both Kr and Ar, with Kr yielding slightly higher values due to its greater mass and momentum transfer efficiency. Iron shows a similar trend, with higher sputtering yields for Kr than Ar, as seen in the datasets from Weijsenfeld[33] and Rosenberg.[34] The lack of comprehensive stainless steel data remains a pressing issue, mainly because many vacuum chamber testing facilities utilize stainless steel, emphasizing the need for further studies in this area. The systematic differences in yields highlight the influence of ion mass and experimental conditions on sputtering behavior. Moreover, Oyarzabal's[35] work reveals that as the mass of the incident ions increases, the sputtering process for carbon-based materials tends more towards cluster preferential erosion, and carbon clusters are ejected more frequently than individual atoms, which is not preferred for lower mass ions like that of Ar and individual carbon atoms are ejected.

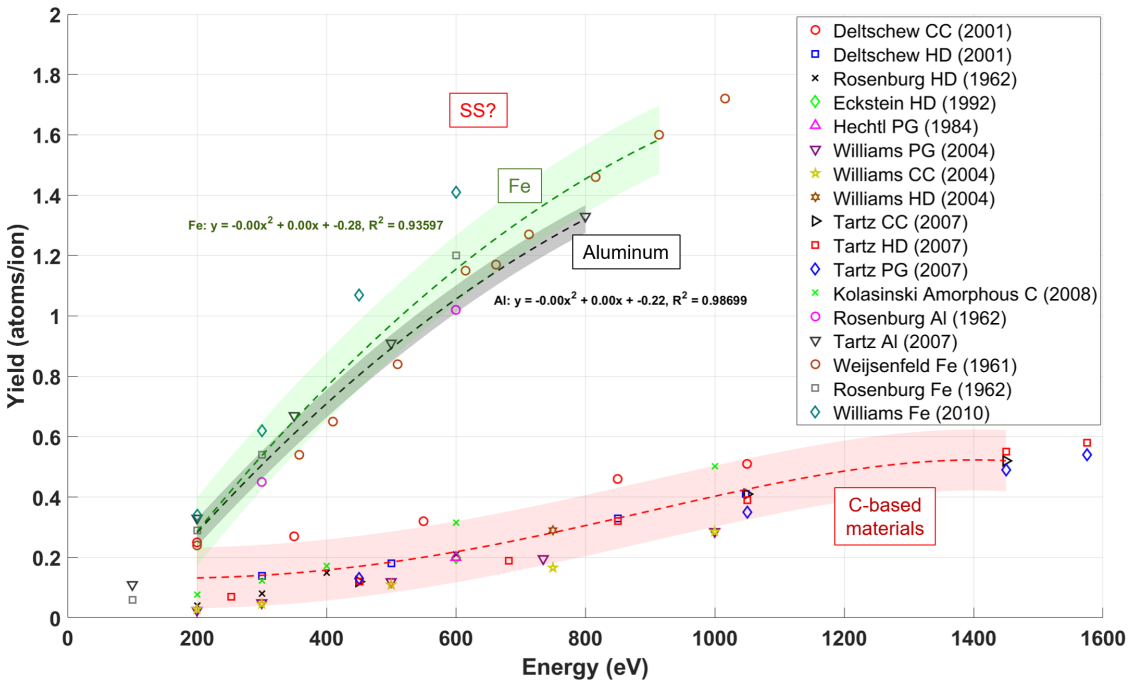

Figure 2: Xenon ion bombardment at normal incidence as a function of ion energy.

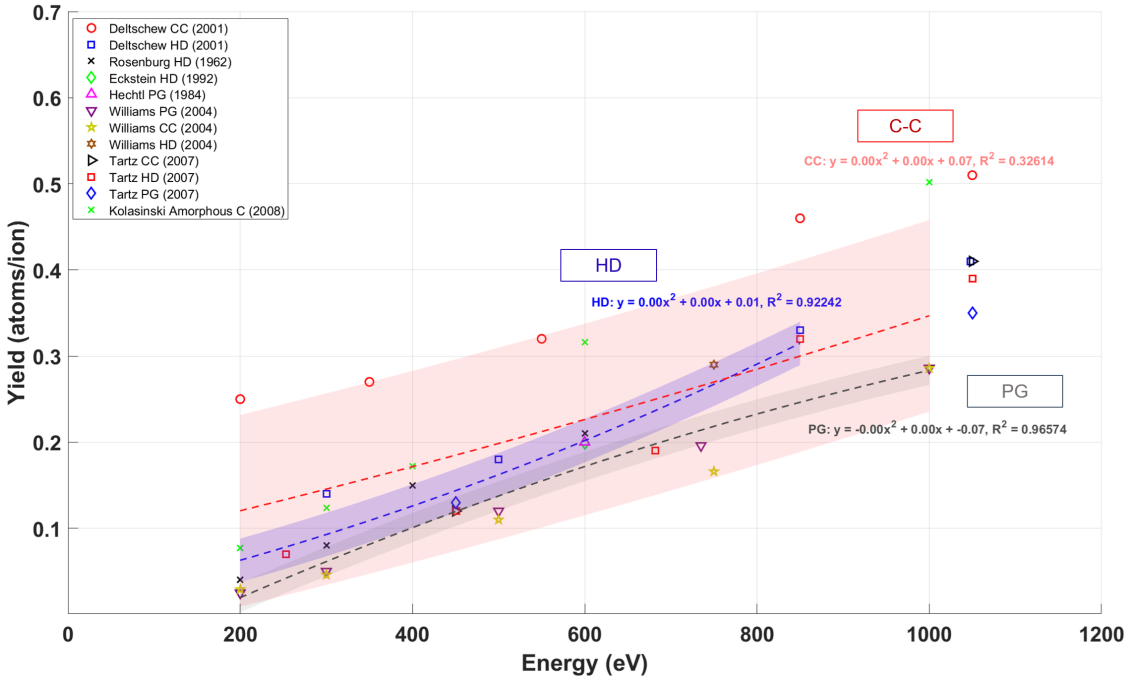

Figure 3: Xenon ion bombardment at normal incidence as a function of ion energy for only C-based materials.

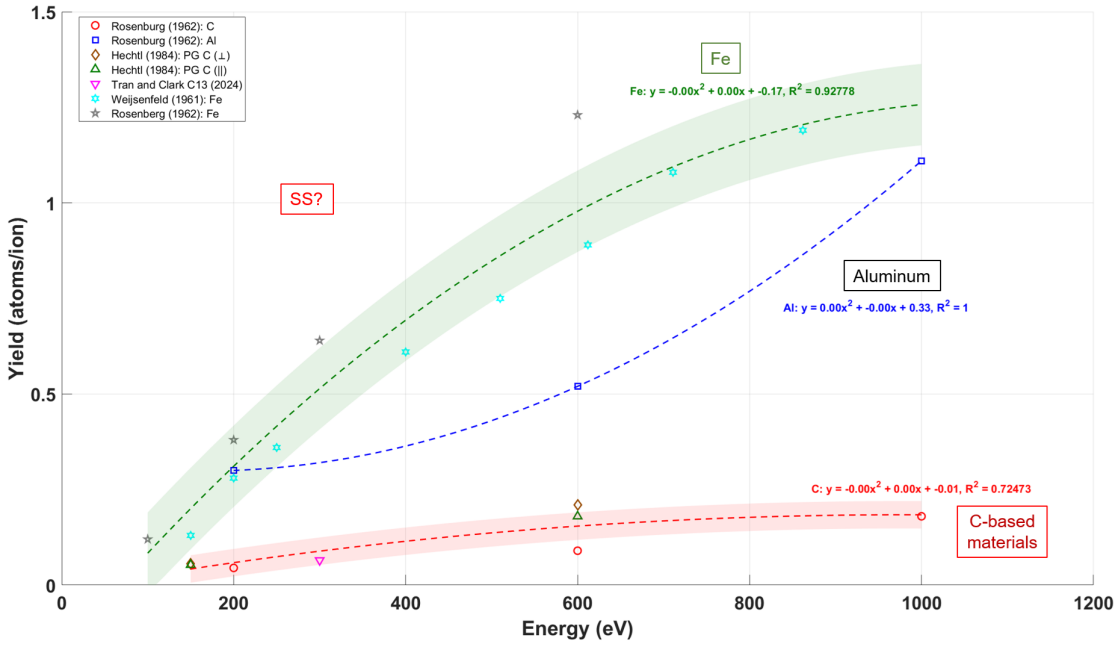

Figure 4: Krypton ion bombardment at normal incidence as a function of ion energy.

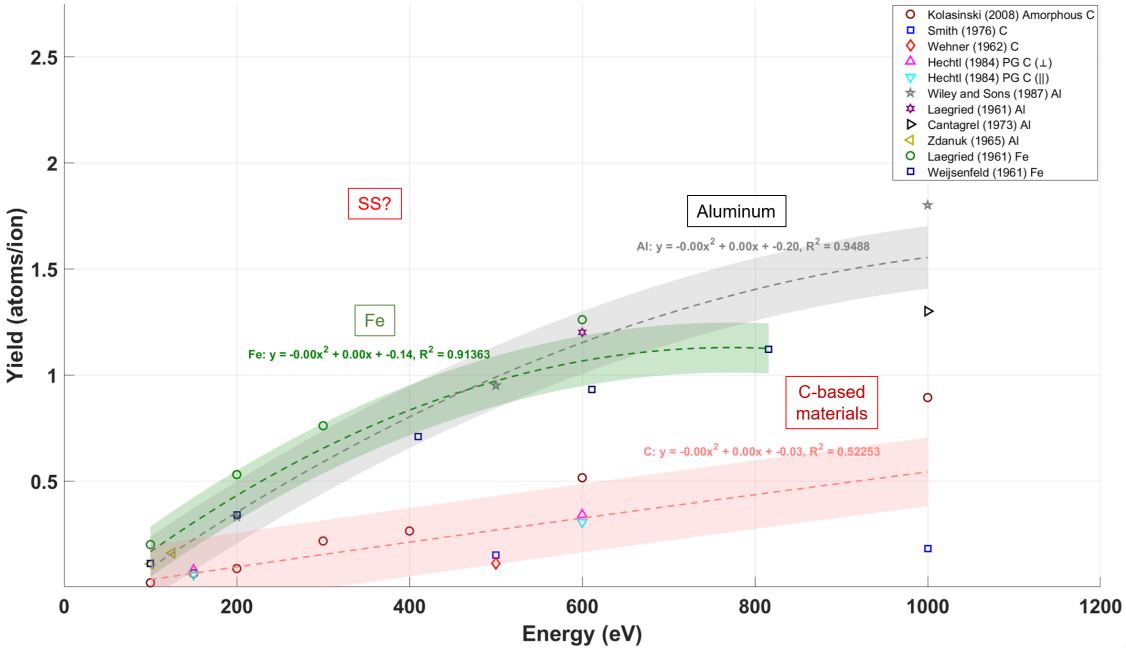

Figure 5: Argon ion bombardment at normal incidence as a function of ion energy.

B. Angular Incidence

Figures 6 and 7 show that sputtering yields for Xe and Kr ions increase with the angle of incidence, peaking at oblique angles due to a balance between energy deposition and recoil atom depth travel, as explained by Wei (2008).[36,37] Notably, no data exists for Ar ion bombardment except for diamond. The angular dependence of preferential sputtering also affects the composition of Al-Cu thin films, emphasizing the need for detailed studies to optimize material performance under ion bombardment.

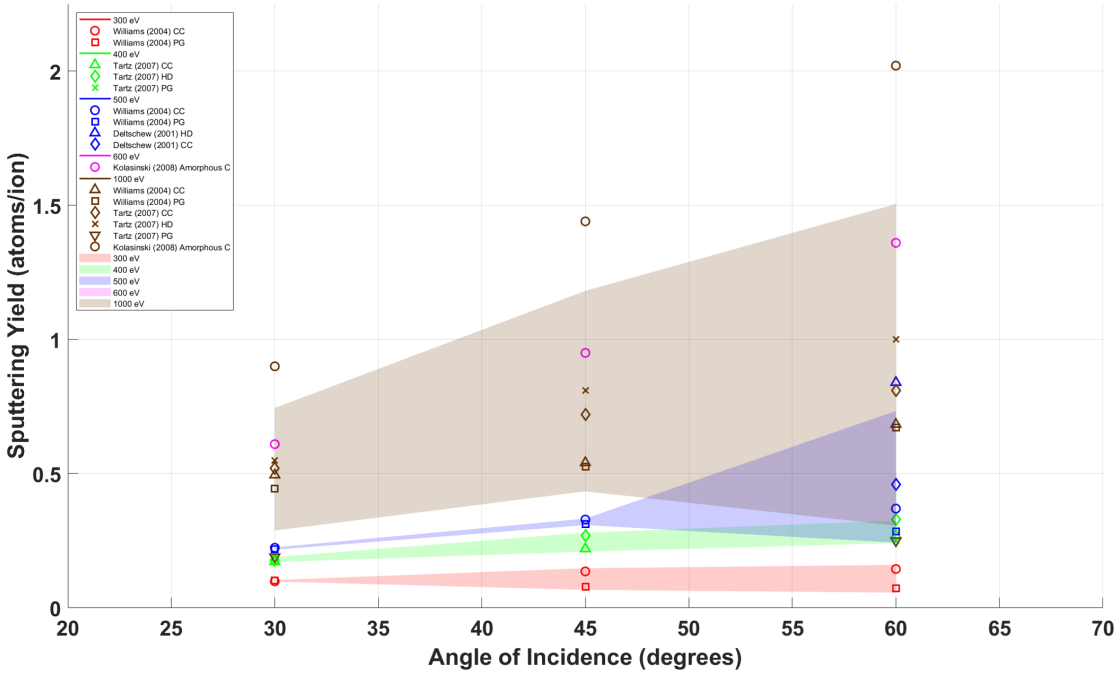

Figure 6: Xe ion bombardment at angular incidence as a function of ion energy.

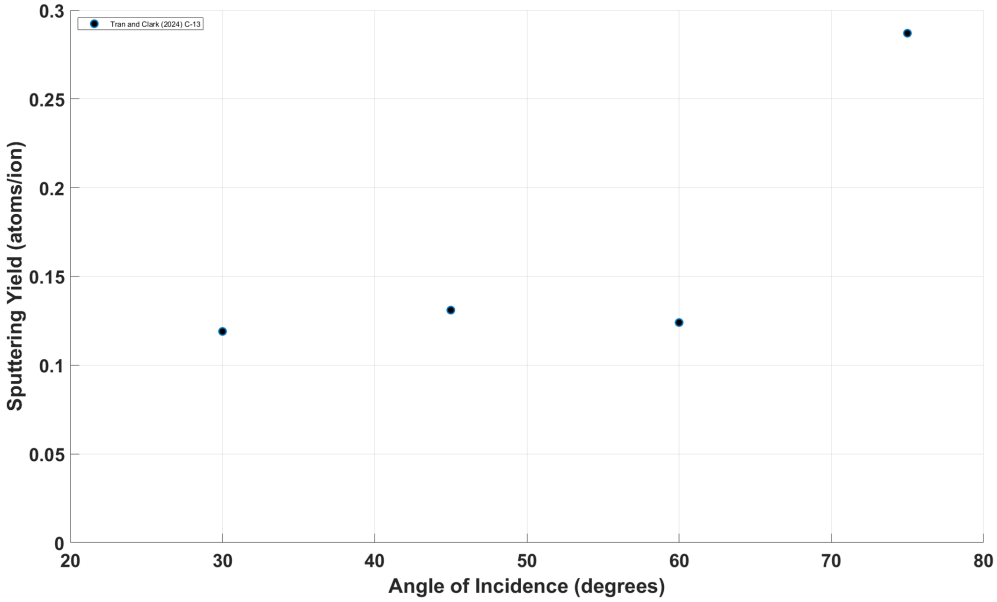

Figure 7: Kr ion bombardment at angular incidence as a function of ion energy.

IV. Conclusion

The following matrix, 8, provides a summary of available data on sputtering yields for xenon, krypton, and argon incident upon carbon, stainless steel, and aluminum. It shows that the most extensive data is available for xenon on carbon, particularly at a 0° angle of incidence, with additional data available for various angles and different types of carbon materials. Limited data is available for krypton, especially at angles other than 0°. Sputtering of argon on carbon has been well-studied at normal incidence but has sparse data for angular dependence. The literature shows a significant gap in sputtering data for stainless steel across all propellants. As for aluminum, there is limited data for xenon, minimal data for krypton at 0° and none at other angles, and well-studied sputtering of argon at normal incidence, but lacking data for energies below 1 keV. The primary conclusion from our discussion of the reduced order model for sputtering is that sputtering profiles for a wide range of angular incidence is paramount to understanding intersurface sputtering and deposition behavior.

Material → Propellant ↓	**Carbon**	**Stainless Steel**	**Aluminum**
Xe	•Most data at **0°** (normal incidence) •Some data at angles •Multiple C material types with different results.	No Sputtering Data available.	Limited sputtering data available
Kr	• $\boldsymbol{\theta = 0°}$: Limited data • $\boldsymbol{\theta \neq 0°}$: Very limited data	No Sputtering Data available.	• $\boldsymbol{\theta = 0°}$: Limited sputtering data available • $\boldsymbol{\theta \neq 0°}$: No sputtering data available. Scientific studies have been done on crystal formation.
Ar	• $\boldsymbol{\theta = 0°}$: Well studied in science community • $\boldsymbol{\theta \neq 0°}$: Data on diamond. Else, very sparse data on sputtering yield due to angular incidence of ions	No Sputtering Data available.	• $\boldsymbol{\theta = 0°}$: Well-studied in science community • $\boldsymbol{\theta \neq 0°}$: No Al data within 1 keV. Scientific studies have been done on crystal formation or Cu-Al alloys

Figure 8: Summary of EP-relevant sputtering for a range of propellants and facility surfaces.

Overall, this analysis highlights the need for more research, via data and models, for EP-relevant facility surface sputtering and deposition. Angular dependence of sputtering yields and sputtering profiles for all relevant materials are needed, as well as the sputtering of deposited materials. Stainless steel sputtering is a particularly unexplored area of research, though all materials need additional studies to fill data gaps or to provide adequate certainty. We encourage any researcher with unpublished or limitedly available data to please make these data available to the community. We note that methods such as Residual Gas Analyzers (RGAs) to monitor species flux from different parts of the chamber will help improve the understanding of the facility material sputtering environment. Lastly, as discussed by Crandall and Wirz[38] and many other groups, alternative propellants are becoming increasingly attractive for new EP applications and should thus be part of an expanding conversation of EP PMI that is beyond the scope of this current work.

Acknowledgments

The authors fully acknowledge support from the Joint Advanced Propulsion NASA Space Technology Research Institute. This work was funded by Joint Advanced Propulsion Institute 20-STRI-FULL-0004, NASA Grant Number 80NSSC21K1118.

References

[1]A. Sengupta, J. Brophy, J. Anderson, C. Garner, B. Banks, and K. Groh. An overview of the results from the 30,000 hr life test of deep space 1 flight spare ion engine. In *40th AIAA/ASME/SAE/ASEE Joint Propulsion Conference and Exhibit*, July 2004. AIAA 2004-3608.

[2]K. de Groh, B. Banks, and C. Karniotis. Nstar extended life test discharge chamber flake analyses. In *40th AIAA/ASME/SAE/ASEE Joint Propulsion Conference and Exhibit*, July 2004. AIAA 2004-3612.

[3]J. E. Polk. The effect of carbon deposition on accelerator grid wear rates in ion engine ground testing. In *36th*

AIAA/ASME/SAE/ASEE Joint Propulsion Conference and Exhibit. American Institute of Aeronautics and Astronautics, 2000.

[4]G. Williams, T. Haag, J. Foster, J. Van Noord, S. Malone, T. Hickman, and M. Patterson. Analysis of the pyrolytic graphite ion optics following the 2000-hour wear test of the hipep ion thruster. In *42nd AIAA/ASME/SAE/ASEE Joint Propulsion Conference & Exhibit*. American Institute of Aeronautics and Astronautics, 2006.

[5]M. Tartz and H. Neumann. Sputter yields of carbon materials under xenon ion incidence. *Plasma Processes and Polymers*, 4:S633–S636, 2007.

[6]Robert B Lobbia, James E Polk, Richard R Hofer, Vernon H Chaplin, and Benjamin Jorns. Accelerating 23,000 hours of ground test backsputtered carbon on a magnetically shielded hall thruster. In *AIAA Propulsion and Energy 2019 Forum*, page 3898, 2019.

[7]S. Hu, A. Joshi, V. Khayms, B. Emgushov, L. Werthman, and V. Smentkowski. Hall thruster plume effects and sputtering of spacecraft surfaces. In *37th Joint Propulsion Conference and Exhibit*, July 2001. AIAA 2001-3356.

[8]R. R. Hofer, B. A. Jorns, J. E. Polk, I. G. Mikellides, and J. S. Snyder. Wear test of a magnetically shielded hall thruster at 3000 seconds specific impulse. In *33rd International Electric Propulsion Conference*, The George Washington University, Washington, D. C., October 2013. IEPC-2013-033.

[9]James E Polk, Vernon Chaplin, John Yim, George Soulas, George Williams, and R Shastryk. Modeling ion optics erosion in the next ion thruster using the cex2d and cex3d codes. In *36th International Electric Propulsion Conference*, 2019.

[10]Richard E Wirz, John R Anderson, and Ira Katz. Time-dependent erosion of ion optics. *Journal of Propulsion and Power*, 27(1):211–217, 2011.

[11]Christopher M. Cretel and Richard E. Wirz. Ion thruster grid life and performance prediction via reduced order modeling. In *38th International Electric Propulsion Conference*, pages IEPC–2024–758, 2024.

[12]Graeme Sabiston and Richard E. Wirz. Electric propulsion vacuum chamber design approaches for reducing sputtering effects. In *38th International Electric Propulsion Conference*, pages IEPC–2024–187, 2024.

[13]Ryan W. Cowan, Saptarshi Biswas, Luke K. Franz, Chris M. Cretel, Richard A. Obenchain, and Richard E. Wirz. Het erosion and deposition for facility surfaces. In *38th International Electric Propulsion Conference*, Pierre Baudis Convention Center, Toulouse, France, June 2024. IEPC-2024-549.

[14]Luke K. Franz and Richarz Wirz. Xe-c scattering, implantation, and sputtering analysis for ep systems. In *38th International Electric Propulsion Conference*, pages IEPC–2024–552, 2024.

[15]Charles Lipscomb, Iain D Boyd, Kaelan B Hansson, Joshua Eckels, and Alex Gorodetsky. Simulation of vacuum chamber pressure distribution with surrogate modeling and uncertainty quantification. In *AIAA SCITECH 2024 Forum*, page 2369, 2024.

[16]Ehsan Taghizadeh, Richard A. Obenchain, Luke K. Franz, and Richard Wirz. Electric propulsion facility optimization via reduced order modeling. In *38th International Electric Propulsion Conference*, pages IEPC–2024–558, 2024.

[17]J. E. Polk. A critical review and meta-analysis of xenon-on-carbon sputter yield data. *Journal of Applied Physics*, 135(4):040701, 2024.

[18]I. D. Boyd and M. L. Falk. A review of spacecraft material sputtering by hall thruster plumes. In *37th Joint Propulsion Conference*, Salt Lake City, Utah, July 2001. AIAA Paper 2001-3353.

[19]John T. Yim. Overview of the joint advanced propulsion institute (janus). In *35th International Electric Propulsion Conference*, pages IEPC–2017–060, 2017.

[20]E. Hecht and J. Bohdansky. Sputtering behavior of graphite and molybdenum at low bombarding energies. *Journal of Nuclear Materials*, 122 and 123:1431–1436, 1984.

[21]V. I. Shulga. Title of the paper. *Radiation Effects and Defects in Solids*, 172:610, 2017.

[22]H. Tran and H.B. Chew. Surface morphology and carbon structure effects on sputtering: Bridging scales between molecular dynamics simulations and experiments. *Carbon*, 2023.

[23]M. Nakano, S. Hosoda, and K. Nishiyama. Title of the paper. *Transactions of The Japan Society for Aeronautical and Space Sciences*, 58:213, 2015.

[24]M. S. Dresselhaus and R. Kalish. *Ion Implantation in Diamond, Graphite and Related Materials*, volume 22 of *Springer Series in Materials Science*. Springer-Verlag, 1992.

[25]D. Marton, K.J. Boyd, T.E. Lytle, and J.W. Rabalais. Auger electron spectroscopy of krypton subplanted in graphite. *Surface Science*, 282:113–121, 1993.

[26]John D. Williams and Ronald L. Corey. Influence of residual gases on witness plate measurements during hall-effect thruster testing. *Plasma Sources Science and Technology*, 19:025020, 2010.

[27]H. Tran, S. Clark, R. Thompson, D.A. Levin, J. Rovey, and H.B. Chew. Carbon transport in electric propulsion testing – i: Multiscale computations for carbon sputtering by low energy ion bombardment. In *AIAA SciTech Forum*, Orlando, FL, January 2024.

[28]Ryan W. Cowan, Saptarshi Biswas, Luke K. Franz, Christopher M. Cretel, Richard A. Obenchain, and Richard E. Wirz. Hall thruster krypton sputtering effects on vacuum facility materials. In *38th International Electric Propulsion Conference*, pages IEPC–2024–549, 2024.

[29]John Williams, Mark Johnson, and Desiree Williams. Differential sputtering behavior of pyrolytic graphite and carbon-carbon composite under xenon bombardment. In *40th AIAA/ASME/SAE/ASEE Joint Propulsion Conference and Exhibit*, page 3788, 2004.

[30]H Tran and HB Chew. Surface morphology and carbon structure effects on sputtering: Bridging scales between molecular dynamics simulations and experiments. *Carbon*, 205:180–193, 2023.

[31]R. Deltschew, M. Tartz, V. Plicht, E. Hartmann, H. Neumann, H. J. Leiter, and J. Esch. Sputter yield measurements of graphite and carbon-carbon material for ion thruster grids. In *37th AIAA/ASME/SAE/ASEE Joint Propulsion Conference and Exhibit*, Salt Lake City, Utah, July 2001. American Institute of Aeronautics and Astronautics. (c)2001 American Institute of Aeronautics & Astronautics or Published with Permission of Author(s) and/or Author(s)' Sponsoring Organization.

[32]Robert D. Kolasinski, James E. Polk, Dan Goebel, and Lee K. Johnson. Carbon sputtering yield measurements at grazing incidence. *Journal of Applied Physics*, 102(10):103301, May 2007. Received 3 May 2007; accepted 26 September 2007; Available online 2 October 2007.

[33]C. H. Weijsenfeld, A. Hoogendoorn, and M. Koedam. Sputtering of polycrystalline metals by inert gas ions of low energy (100- 1000 ev). *Physica*, 27(8):763–764, 1961.

[34]D. Rosenberg and G. K. Wehner. Sputtering yields for low energy he+, kr+, and xe+ ion bombardment. *Journal of Applied Physics*, 33(5):1842–1845, 1962. Published by the American Institute of Physics.

[35]E. Oyarzabal, R. P. Doerner, M. Shimada, and G. R. Tynan. Carbon atom and cluster sputtering under low-energy noble gas plasma bombardment. *Journal of Applied Physics*, 104(4):043305, 2008.

[36]Qiangmin Wei, Kun-Dar Li, Jie Lian, and Lumin Wang. Angular dependence of sputtering yield of amorphous and polycrystalline materials. *Journal of Physics D: Applied Physics*, 41(17):172002, 2008.

[37]Peter Sigmund. Theory of sputtering. i. sputtering yield of amorphous and polycrystalline targets. *Physical Review*, 184(2):383, 1969.

[38]Patrick Crandall and Richard E Wirz. Miniature rf gridded ion thruster for air-breathing ep. In *38th International Electric Propulsion Conference*, pages IEPC–2024–259, 2024.